ISSN 1067-8212, Russian Journal of Non-Ferrous Metals, 2018, Vol. 59, No. 6, pp. 685–692. © Allerton Press, Inc., 2018.
Original Russian Text © Yu.R. Kolobov, A.N. Prokhorov, S.S. Manokhin, A.Yu. Tokmacheva-Kolobova, D.I. Serebryakov, V.V. Afanasiev, 2018, published in Izvestiya Vysshikh Uchebnykh Zavedenii, Poroshkovaya Metallurgiya i Funktsional'nye Pokrytiya, 2018, No. 3, pp. 76–86.

MATERIALS AND COATINGS FABRICATED BY ADDITIVE TECHNOLOGIES

Comparative Study of the Structural-Phase State and Mechanical Properties of Ni–Cr(X) and Fe–Cr(X) Heat-Resistant Alloys Fabricated by Additive Technologies

Yu. R. Kolobov[a, b, c, *], A. N. Prokhorov[d, **], S. S. Manokhin[a, b, *], A. Yu. Tokmacheva-Kolobova[a, e, ****], D. I. Serebryakov[d, *****], and V. V. Afanasiev[d]**

[a] *Institute of Problems of Chemical Physics, Russian Academy of Sciences, Chernogolovka, Moscow oblast, 142432 Russia*
[b] *Belgorod State National Research University, Belgorod, 308034 Russia*
[c] *Moscow State Univerisity, Moscow, 119991 Russia*
[d] *Central Institute of Aviation Motors (CIAM), Moscow, 111116 Russia*
[e] *National University of Science and Technology "MISiS", Moscow, 119049 Russia*
**e-mail: kolobov@bsu.edu.ru*
***e-mail: prokhorov@ciam.ru*
****e-mail: manohin@bk.ru*
*****e-mail: anastasiia.misis@gmail.com*
******e-mail: serebryakov012@ciam.ru*

Received May 30, 2018; in final form, July 20, 2018; accepted for publication July 23, 2018

Abstract—Comparative studies of peculiarities of the formation, thermal stability of the structure, and mechanical properties of heat-resistant alloys based on iron and nickel and fabricated using additive technologies (ATs) by laser metal deposition and selective laser melting are performed. It is established that a cellular structure is formed in alloys fabricated by the laser metal deposition and small pores up to 200 nm in size are present. The structure of alloys fabricated by selective laser melting contains elements with a globular and lamellar morphology and incompletely melted regions, as well as large pores on the order of 5 μm in size. The possibility of manifestation of the nanophase hardening effect due to the presence of nanodimensional particles of chromium silicides is shown. A comparative analysis of mechanical properties of materials under study is performed. It is shown that iron-based alloys possess higher strength and lower ductility when compared with nickel alloys. All studied samples fabricated by selective laser melting have higher strength characteristics when compared with alloys fabricated by laser metal deposition. Short-term annealing at 900–1000°C for 1 h noticeably decreases both strength and plasticity in tensile and compression tests at room and elevated temperatures. Alloys based on iron and nickel fabricated by laser metal deposition and subjected to compression tests at $t = 900$°C have similar strength characteristics. In contrast with iron-based alloys, additional annealing of the nickel-based AT alloy almost does not decrease its strength characteristics.

Keywords: heat-resistant alloys, additive technologies, structure, phase composition
DOI: 10.3103/S1067821218060111

INTRODUCTION

Currently, materials fabricated using new additive technologies (ATs) are actively studied and find broad application in various fields of technology and medicine. ATs open up possibilities of producing three-dimensional complexly shaped metallic articles according to a specified computer model by the layer-by-layer deposition of the powder material into the melting zone and the subsequent or simultaneous effect of laser irradiation.

It is known that especially high requirements are demanded for materials for the fabrication of parts of aircrafts and space vehicles, which are subjected to the simultaneous effect of high temperatures and mechanical loads during operation [1–3]. Heat-resistant alloys based on nickel and iron of Ni–Cr(X) and Fe–Cr(X) systems, for example, domestic alloys of VZh98 and VZh171 grades and foreign alloys Inconel 625, Inconel 714, etc., have been applied in technology for many decades because they have a thermally stable structure, and characteristics of strength, corrosion resistance, and creep resistance at usual, elevated, and high temperatures improved when compared with traditional materials. The phase composition of such alloys is presented by a nickel/iron-based alloyed solid solution with particles of secondary phases. It is known that particles of dispersed secondary phases

(carbides, nitrides, oxides, etc.), which are arranged at grain boundaries, increase the high-temperature strength of metallic polycrystals because they prevent the migration of grain boundaries and development of recrystallization and grain-boundary sliding under conditions of the simultaneous effect of temperature and load [2].

Many occurring and well-studied heat-resistant alloys are tough-to-machine; therefore, improving the production technology of complexly shaped parts by AT methods seems to be an important task [4]. Data have been published on comparable or even higher strength characteristics of room-temperature tensile and compression tests of heat-resistant alloys synthesized using AT when compared with cast and deformed alloys [5, 6]. At the same time, there is scant information on the behavior of AT alloys under cyclic loading conditions. The manifestation of improved mechanical properties is associated with high anisotropy of AT alloys in view of the possibility for the precision control of the growth direction and shape of structural elements of such materials [7].

The authors of [8] showed that mechanical properties of the Inconel 718 alloy fabricated by laser metal deposition in tensile tests are comparable with corresponding characteristics for cast and deformed alloys. However, the plasticity and rupture stress of the samples of AT alloys are substantially lower than similar mechanical properties for samples made of cast and deformable billets, mainly due to the presence of porosity. The strength characteristics of the Inconel 718 AT alloy subjected to hot isostatic pressing in tensile tests exceed the corresponding characteristics for the deformed alloy because the AT alloy has the smaller grain size. Herewith, similarly to the data [8], the AT material manifests lower plasticity when compared with the deformed material.

Despite the many clear advantages of AT methods, they are currently unable to replace traditional metallurgical technologies in view of a series of definite difficulties. For example, a common problem for all materials produced using AT methods is the presence of defects such as pores and incomplete fusion zones [9]. It is known that two types of porosity are distinguished in AT alloys [10]:

(i) spherical pores formed due to gas absorption during powder preparation and unfused regions;

(ii) shrinkage defects appearing during fabrication, which usually have a spherical shape and large size.

The morphology and defect distribution over the sample bulk are studied in detail using X-ray computer tomography in [11] by the example of the Ti–6Al–4V alloy fabricated by selective laser sintering. Pores, inside which incompletely fused particles of initial powder are met, are shaped like discs 100–200 μm in diameter and are distributed nonuniformly over the material bulk. Possible causes of pore formation during material fabrication using this method are investigated in [12], where it was assumed that pore formation is associated with the instability of the melt flow and molten material spraying.

The authors of [13] attribute the formation of spherical pores smaller than 10 μm in diameter in the Ti–6Al–4V alloy fabricated by electron-beam selective melting to the isolation of bubbles of inert gas absorbed by metal powder during its synthesis. Herewith, the larger part of pores in the material is concentrated near the surface, where large pores ~50 μm in size are also observed. The authors of [6] note that the larger part of pores in the Inconel 718 alloy fabricated by laser metal deposition is arranged in a near-surface layer with a thickness of about 2 mm, which can be easily removed mechanically.

The presence of internal defects negatively affects the strength of materials fabricated using ATs under cyclic loading because it facilitates the nucleation and propagation of the main crack. The authors of [14] found that the inhomogeneity of the formed structure, notably the grain elongation along the growth direction, and the presence of residual stresses appearing because of a large temperature gradient during melting affect the multicycle fatigue. Nevertheless, the mechanical characteristics of AT alloy under the multicycle fatigue comparable with corresponding characteristics of deformed and cast alloys are given in certain publications [15]. According to the data [9], the presence of porosity leads to a decrease in the fatigue limit of the AT alloy when compared with the deformed analog alloy during low-cycle tests. For example, the Inconel 718 alloy fabricated by laser metal deposition has a larger fatigue limit when compared the deformed alloy when the deformation amplitude lies in a range from 0.6 to 0.8%. With an increase in the latter to 1.0%, the deformed alloy has a larger fatigue limit.

In order to decrease the porosity in the bulk and on the material surface, various methods of treatment are used such as hot isostatic pressing and cathode-arc deposition [16, 17]. According to [17], the fatigue properties of the Inconel 718 alloy subjected to the abovementioned types of treatment worsen regardless of the performance of additional annealing (t = 1000°C, τ = 1 h). The authors of [9] explain the decrease in the fatigue limit of this ally under cyclic tests with the formation of numerous annealing twins during hot isostatic pressing.

There is a series of experimental works devoted to investigating the temperature dependence of the mechanical properties of AT materials in the literature. The authors of [18] studied the mechanical characteristics of the Inconel 718 alloy fabricated by laser metal deposition during compression tests in a temperature range from 940 to 1060°C. It was found that the yield points for alloys fabricated using ATs and by methods of traditional metallurgy have similar values.

The goal of this study is to compare the forming structure, phase composition, and mechanical properties of heat-resistant alloys of Ni–Cr(X) and Fe–Cr(X) systems fabricated by laser metal deposition and selective laser melting.

EXPERIMENTAL

We selected samples of nickel-based alloys of the Ni–Cr(X) system (the Russian analog of the foreign Inconel 718 alloy) and iron-based alloys of the Fe–Cr(X) system (the Russian analog of the foreign AISI 304 heat-resistant steel) fabricated using ATs (by laser metal deposition and selective laser melting) and presented by CIAM (Moscow).

The chemical composition of mentioned materials determined by X-ray spectral microanalysis is presented in Tables 1 and 2.

Slices for metallographic investigations were prepared using a LaboPol-5 installation (Struers). The samples were annealed in Nabertherm laboratory furnaces.

The alloy microstructure was investigated by optical microscopy (an Olympus GX41 microscope) and transmission electron microscopy (TEM) using a Tecnai G2 F20 S-TWIN microscope under an accelerating voltage of 200 kV (including the scanning transmission electron microscopy mode), as well as scanning electron microscopy (SEM) using Quanta 600 FEG, NovaNanoSem 450, and Aspex Express FEI field-emission high-resolution scanning electron microscopes under accelerating voltages of 20 and 30 kV. The energy-dispersive elemental microanalysis was performed using an attachment produced by EDAX and TecnaiImaging&Analysis software. The samples of the specified shape were cut using an AQ300L spark-erosion installation.

The X-ray structural investigations were performed using an ARL X'TRA diffractometer (Thermo Fisher Scientific) under the following conditions: CuK_α radiation (λ = 1.5406 Å), the scanning step is 0.02°, the angle range is $2\theta = 30°–132°$, and the exposure is 1 s. The X-ray diffraction patterns were processed using the PDXL 2 software and the phase composition was determined using the ICDD-2003 database.

Tensile tests with a strain rate of 1×10^{-3} s^{-1} were performed using an Instron 3883 universal testing machine and compression tests were performed using an Instron 300 machine. The tensile samples were shaped like two-bladed vanes, the working part of which had sizes 16 × 3 × 1.5 mm for room-temperature tests and 35 × 7 × 2 mm for high-temperature tests. The samples for high-temperature compression tests were shaped like parallelepipeds 6 mm in height with the base 3 × 3 mm in size. Three samples were investigated in each series of experiments.

Table 1. Chemical composition of the alloy of the Ni–Cr(X) system

Measurement units	Ni	Cr	Fe	Nb	Mo	Ti	Al
wt %	52.48	19.15	18.10	4.93	3.61	1.02	0.73
at %	51.82	21.35	18.79	3.07	2.18	1.23	1.56

Table 2. Chemical composition of the alloy of the Fe–Cr(X) system

Measurement units	Fe	Cr	Ni	Mo	Si
wt %	66.51	19.92	9.96	2.51	1.09
at %	65.84	21.18	9.38	1.44	2.15

RESULTS AND DISCUSSION

Alloy of the Fe–Cr(X) System

The structure of the alloy fabricated by laser metal deposition is inhomogeneous by bulk in the delivery state. Elongated and rounded traces of the laser beam are observed in the longitudinal and transverse sections according to the optical metallography data. The sample structure in the transverse section (Fig. 1a), which is revealed using a metallographic microscope, consists of melt crystallization baths shaped like circle segments. Its arc, as was shown in [19], is the crystallization front, while the radius depends on the temperature gradient, i.e., on laser-beam energy parameters.

Certain regions of the alloy under study have a cellular microstructure with a size of structural elements of 0.5–1.0 μm (Fig. 1b), which is usually observed in AT alloys [20]. It seems likely that the cellular-structure formation is associated with sequentially proceeding melting and crystallization upon material heating by the laser beam during synthesis and subsequent cooling. Pores up to 0.2 μm in size are observed at cell boundaries. In view of the presence of $CrSi_2$ particles ~50 nm in size in the austenite matrix (Fig. 1b), the possibility of implementing the known effect of nanophase hardening is assumed. The structure contains pores 5 μm in size and larger, as well as regions of an incompletely fused mixture of particles of initial powder, the average size of which is ~30 μm (Fig. 2).

Microstructural elements in a form of strips of about 1–3 μm in width (Fig. 3) and numerous extinction contours evidencing the presence of large internal stresses are observed in the alloy fabricated by selective laser melting, in contrast with the sample fabricated by laser metal deposition. In addition, similarly to the alloy fabricated by laser metal deposition, it contains inclusions of nanodimensional particles of the second phase ~50 nm in size.

The alloy under study fabricated by laser metal melting annealed at 1000°C for 1 h has a room-tem-

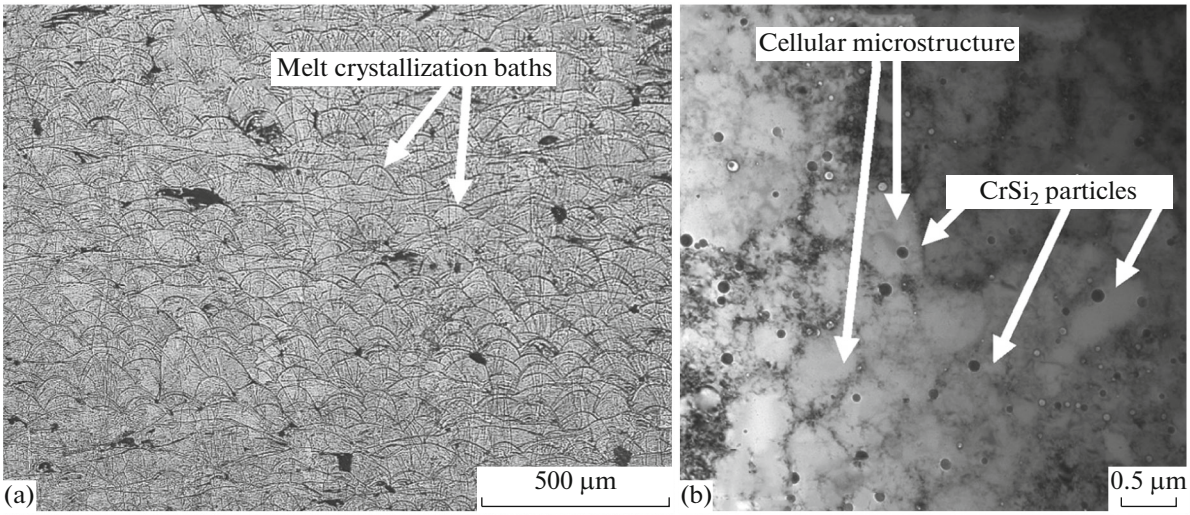

Fig. 1. Microstructure of the alloy of the Fe–Cr(X) system fabricated by laser metal deposition. (a) Optical metallography, transverse section, ×100, and (b) transmission electron microscopy.

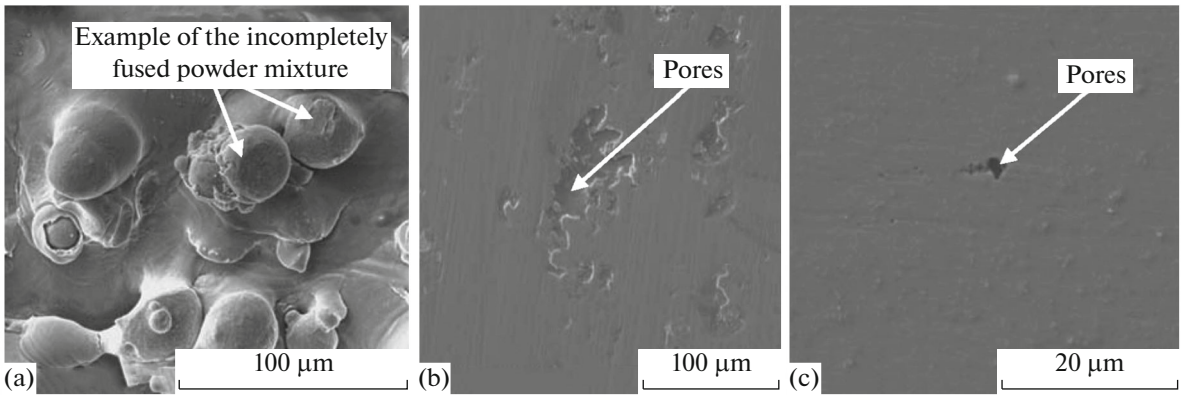

Fig. 2. Typical examples of the region with (a) an incompletely fused mixture of the particles of initial powder and (b, c) porosity in the alloy of the Fe–Cr(X) system fabricated by laser metal deposition (SEM).

perature ultimate strength noticeably lower (by 9–15%) than without annealing and higher plasticity (Fig. 4a).

Annealing at t = 1000°C and τ = 1 h of the iron-based alloy fabricated by selective laser melting (Fig. 4b, Table 3) leads to a decrease in the ultimate strength similarly to the sample fabricated by laser metal deposition. However, no increase in plasticity occurs in this case; however, on the contrary, an essential decrease in the strain before the tensile fracture is observed.

Strength characteristics of the iron-based alloy fabricated by laser metal deposition regularly decrease during compression tests at t = 800–1000°C. Material annealing at t = 1000°C for 1 h does not noticeably affect the yield point and ultimate strength at test temperatures of 900 and 1000°C. A decrease in the alloy

Table 3. Results of room-temperature tensile mechanical tests of the iron-based alloy of the Fe–Cr(X) system fabricated by selective laser melting

Sample state	Strain rate, mm/min	Conditional yield point, MPa	Ultimate strength, MPa	Maximal plastic deformation, %
Initial	2	900 ± 16	1150 ± 23	20 ± 2
After annealing at 1000°C, 1 h	2	840 ± 20	980 ± 45	12 ± 2

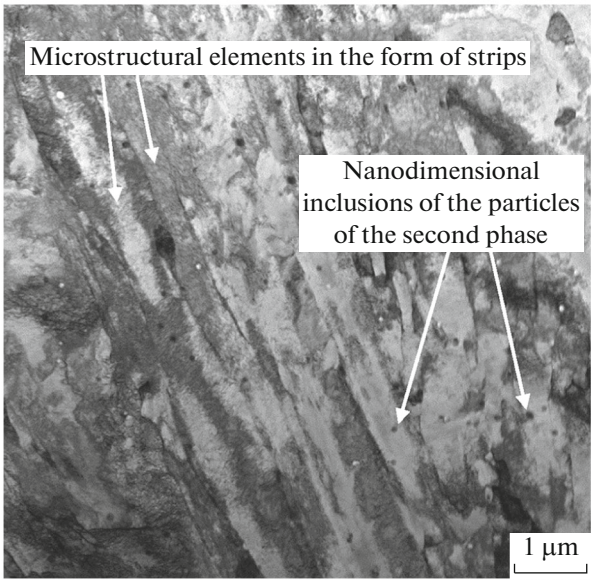

Fig. 3. Microstructure of the Fe–Cr(X) AT alloy fabricated by selective laser melting (TEM).

yield point is observed during compression tests at t = 800°C, while the ultimate strength is independent of this heat treatment. Corresponding mechanical characteristics for the entire studied range of temperatures and states are presented in Table 4.

Alloy of the Ni–Cr(X) System

According to the transmission electron microscopy data, the studied samples of the nickel-based alloy fabricated by laser metal deposition have a cellular structure characteristic of AT materials [20, 21]. Surface defects in the form of pores are observed in certain regions. The main matrix bulk is the nickel-based solid solution with the fcc lattice (lattice parameter a = 3.603 Å), which is confirmed by the results of X-ray structural analysis. Spherical inclusions of the second phase, identified as niobium silicide ~0.5 μm in size, are present in the matrix bulk.

The structure of the sample fabricated by selective laser melting, similarly to the above-considered iron-based alloy, consists of crystallized melt baths (Fig. 5).

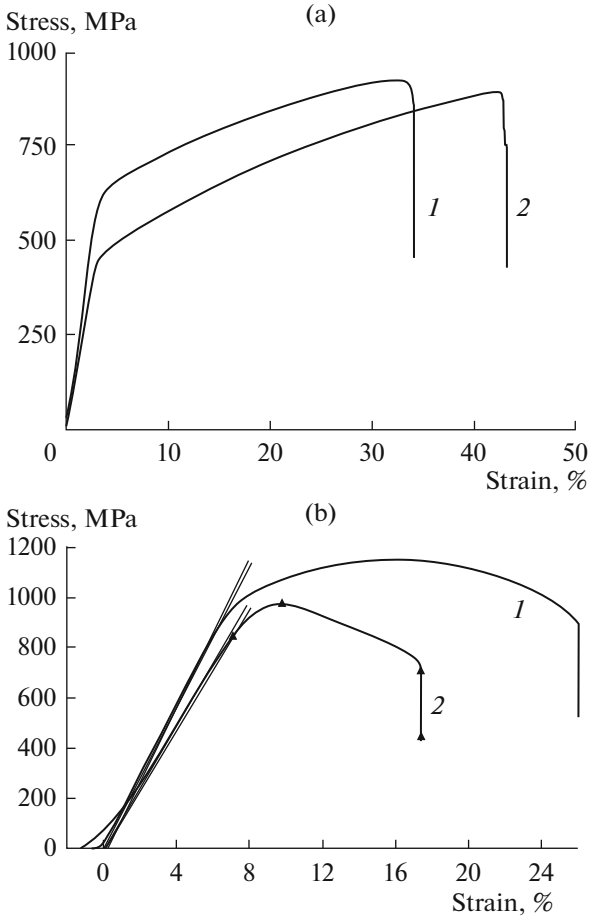

Fig. 4. Strain curves of the iron-based alloy of the Fe–Cr(X) system fabricated by (a) laser metal deposition and (b) selective laser melting during the room-temperature tensile test. (*1*) Initial material and (*2*) material after annealing at t = 1000°C, τ = 1 h.

In general, the material structure is inhomogeneous and regions of the globular and lamellar morphology are observed. It seems likely that they consist of separate polycrystalline grains in both the transverse and longitudinal direction. Pores with a size varying from units to tens of micrometers are present on the sample surface. An incompletely fused mixture of particles of initial power ~30 μm in size is retained in certain local regions. Herewith, the particles of this mixture on the inner surface of the cylin-

Table 4. Mechanical properties of the Fe–Cr(X) alloy fabricated by laser metal deposition during compression tests at elevated temperatures

t, °C	Initial state		Annealing at 1000°C, 1 h	
	yield point, MPa	ultimate strength, MPa	yield point, MPa	ultimate strength, MPa
800	310 ± 16	329 ± 10	217 ± 11	329 ± 20
900	179 ± 20	225 ± 16	170 ± 14	197 ± 9
1000	128 ± 12	132 ± 20	115 ± 10	127 ± 23

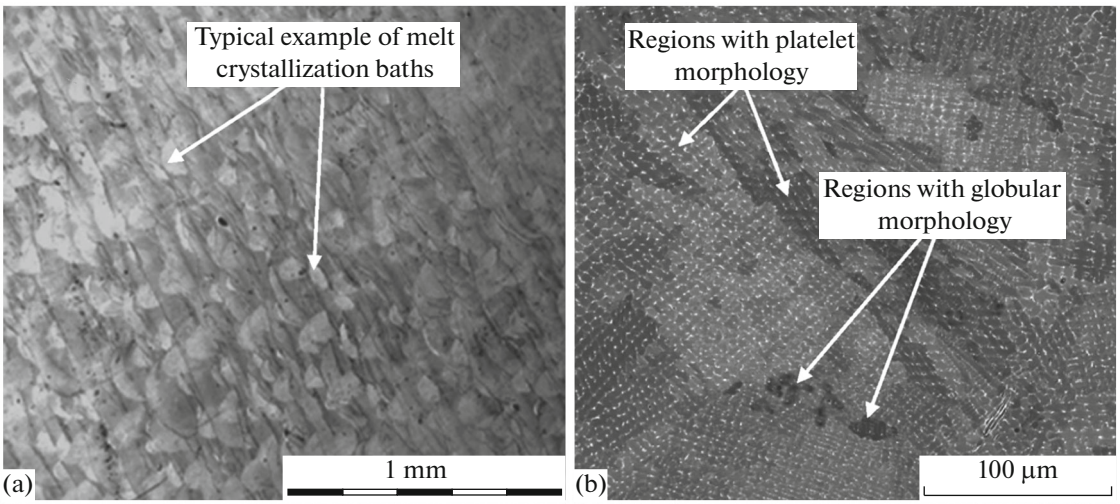

Fig. 5. Microstructure of the alloy of the Ni–Cr(X) system fabricated by selective laser melting (transverse sample section). (a) Optical metallography and (b) scanning electron microscopy.

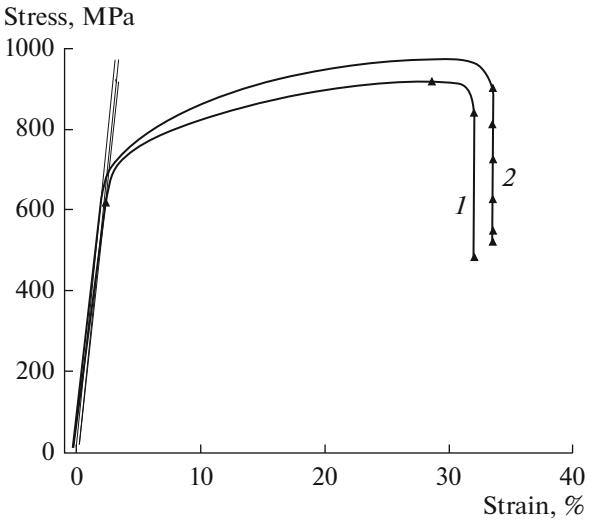

Fig. 6. Strain curves of the alloy samples of the Ni–Cr(X) system fabricated by selective laser melting during the room-temperature tensile test. (*1*) Initial material and (*2*) material after annealing.

drical channel of ready articles can completely or partially overlap them.

An investigation into the mechanical properties of the alloy was performed for the samples fabricated by each of two abovementioned methods in the initial state and subjected to short-term annealing at t = 900–1000°C. It is found that additional annealing of the alloy fabricated by laser metal deposition does not lead to a decrease in strength characteristics during room-temperature tensile tests. It can be seen from Table 5 that an increase in the ultimate strength and fracture strain is observed for the annealed alloy.

An increase in the annealing strength is noted after annealing for the nickel-based sample fabricated by selective laser melting; herewith, the degree of deformation remains almost invariable up to the fracture (Fig. 6, Table 6). It is noteworthy that the plasticity of the above-described iron-based alloy fabricated by selective laser melting is considerably lower in similar conditions than for the nickel-based alloy fabricated by the same method. Room-temperature mechanical properties of the material under study are comparable with corresponding characteristics of Russian and foreign producers.

Strength characteristics of the nickel-based alloy fabricated by laser metal deposition are substantially lower at t = 900°C than at room temperature and close to corresponding value for the iron-based alloy. The mechanical properties of the alloy during the compression tests at t = 900°C are presented in Table 7.

Table 5. Mechanical properties of the alloy of the Ni–Cr(X) system fabricated by laser metal deposition during room-temperature compression tests

Sample state	Yield point, MPa	Ultimate strength, MPa	Degree of strain before the fracture, %
Initial state	442 ± 18	690 ± 20	26 ± 2
After annealing at 1000°C, 1 h	390 ± 16	730 ± 10	42 ± 7

Table 6. Results of room-temperature tensile tests of the alloy of the Ni–Cr(X) system fabricated by selective laser melting

Sample state	Strain rate, min	Conditional yield point, MPa	Ultimate strength, MPa	Degree of strain before the fracture, %
Initial state	2	620 ± 17	920 ± 22	29 ± 4
After annealing at 900°C, 30 min	2	620 ± 11	970 ± 11	30 ± 3

Table 7. Mechanical properties of the alloy of the Ni–Cr(X) system fabricated by laser metal deposition during the compression test at 900°C

Sample state	Yield point, MPa	Ultimate strength, MPa	Degree of strain before the fracture, %
Initial state	171 ± 11	200 ± 19	33 ± 4
After annealing at 1000°C, 1 h	219 ± 14	224 ± 10	32 ± 3

CONCLUSIONS

The main features of the structural-phase state are revealed and the mechanical properties of heat-resistant alloys of Ni–Cr(X) and Fe–Cr(X) systems fabricated by laser metal deposition and selective laser melting are investigated.

The formation of an inhomogeneous cellular structure with the presence of pores up to 200 nm in size at cell boundaries is characteristic of alloys fabricated by laser metal deposition. A qualitatively different structure is formed in the studied alloys during selective laser melting. It is characterized by nonuniformity in sizes of microstructural globular elements and the presence of strips with elongated substructural elements with a thickness of 100 nm and smaller. In addition, the structure contains defects in the form of large pores 5 μm in size and larger, as well as local regions, which consist of incompletely fused particles of the initial powder mixture. Nanodimensional particles of chromium silicides, which can be associated with the nanophase strengthening effect, are found in all studied alloys.

It is established that the strength of studied iron-based alloys (regardless of the material fabrication method) is higher than the strength of nickel-based alloys. Herewith, the latter possess noticeably larger plasticity. All studied samples fabricated by selective laser melting show higher strength characteristics when compared with alloys fabricated by laser metal deposition.

Short-term annealing at 900–1000°C results in the improvement of mechanical properties of nickel-based alloys in contrast with iron-based alloys. Annealing of the latter leads to a decrease in both the strength and plasticity for the material fabricated by laser metal deposition and to a decrease in the ultimate strength with the simultaneous increase in the degree of strain before the fracture for the alloy fabricated by selective laser melting.

Being subjected to compression tests at 900°C, nickel-based and iron-based alloys fabricated by laser metal deposition have similar strength characteristics.

ACKNOWLEDGMENTS

This study was supported by the Program of Basic Research of the Presidium of the Russian Academy of Sciences no. 32 “Nanostructures: Physics, Chemistry, Biology, and Foundations of Technologies” and the Thematic Map of Basic Scientific Research no. 0089-2015-0222 of the Institute of Problems of Chemical Physics of the Russian Academy of Sciences.

REFERENCES

1. Kolobov, Yu.R., Kablov, E.N., Kozlov, E.V., Koneva, N.A., Povarova, K.B., Grabovetckaya, G.P., Buntushkin, V.P., Bazyleva, O.A., Muboyadzhyan, S.A., and Budinovskii, S.A., *Struktura i svoistva intermetallidnykh materialov s nanofaznym uprochneniem* (Structure and Properties of Intermetallic Materials with Nanophase Strengthening), Moscow: MISiS, 2008.
2. Kolobov, Yu.R., *Diffuzionno-kontroliruemye protcessy na granitcakh zeren i plastichnost metallicheskikh polikristallov* (Diffusion-Controlled Processes at Grain Boundaries and Plasticity of Metal Polycrystals), Novosibirsk: Nauka, 1998.
3. Lomberg, B.S., Ovsepian, S.V., Bakradze, M.M., and Mazalov, I.S., High-temperature heat resistant nickel alloys for gas turbine engine parts, in: *Aviatcionnye materialy i tekhnologii: Yubileinyi nauchno-tekhnicheskii sbornik* (Aviation Materials and Technologies. Jubilee Sci.-and-Tech. Collection), Kablov E.N., Ed., Moscow: VIAM, 2012. pp. 52–57.
4. Kablov, E.N., Additive technologies—a dominant feature of the national technology initiative, *Intel. Tekhnol.*, 2015, no. 2, pp. 52–55.
5. Lewandowski, J.J. and Seifi, M., Metal additive manufacturing: A review of mechanical Properties, *Annu. Rev. Mater. Res.*, 2016, vol. 46, no. 1, pp. 151–186.
6. Smith, D.H., Bicknell, J., Jorgensen, L., Patterson, B.M., Cordes, N.L., Tsukrov, I., and Knezevic, M., Microstructure and mechanical behavior of direct metal laser

sintered Inconel alloy 718, *Mater. Charact.*, 2016, vol. 113, pp. 1–9.

7. Wu, M.W., Lai, P.H., and Chen, J.K., Anisotropy in the impact toughness of selective laser melted Ti–6Al–4V alloy, *Mater. Sci. Eng. A*, 2016, vol. 650, pp. 295–299.
8. Zhao, X., Chen, J., Lin, X., and Huang, W., Study on microstructure and mechanical properties of laser rapid forming Inconel 718, *Mater. Sci. Eng. A*, 2008, vol. 478, pp. 119–124.
9. Gribbin, S., Bicknell, J., Jorgensen, L., Tsukrov, I., and Knezevic, M., Low cycle fatigue behavior of direct metal laser sintered Inconel alloy 718, *Int. J. Fatigue*, 2016, vol. 93, pp. 156–167.
10. Sames, W.J., List, F.A., Pannala, S., Dehoff, R.R., and Babu, S.S., The metallurgy and processing science of metal additive manufacturing, *Int. Mater. Rev.*, 2016, vol. 61, no. 5, pp. 315–360.
11. Wu, M.W. and Lai, P.H., The positive effect of hot isostatic pressing on improving the anisotropies of bending and impact properties in selective laser melted Ti–6Al–4V alloy, *Mater. Sci. Eng. A*, 2016, vol. 658, pp. 429–438.
12. Qiu, C., Panwisawas, C., Ward, M., Basoalto, H.C., Brooks, J.W., and Attallah, M.M., On the role of melt f low into the surface structure and porosity development during selective laser melting, *Acta Mater.*, 2015, vol. 96, pp. 72–79.
13. Cunningham, R., Narra, S.P., Ozturk, T., Beuth, J., and Rollett, A.D., Evaluating the effect of processing parameters on porosity in electron beam melted Ti–6Al–4V via synchrotron X-ray microtomography, *JOM*, 2016, vol. 68, no. 3, pp. 765–771.
14. Konecna, R., Nicoletto, G., Kunz, L., and Baca, A., Microstructure and directional fatigue behavior of Inconel 718 produced by selective laser melting, *Proced. Struct. Integr.*, 2016, vol. 2, pp. 2381–2388.
15. Scott-Emuakpor, O., Schwartz, J., George, T., Holycross, C., Cross, C., and Slater, J., Bending fatigue life characterisation of direct metal laser sintering nickel alloy 718, *Fatigue Fract. Eng. Mater. Struct.*, 2015, vol. 38, pp. 1105–1117.
16. Tillmann, W., Schaak, C., Nellesen, J., Schaper, M., Aydinöz, M.E., and Niendorf, T., Functional encapsulation of laser melted Inconel 718 by Arc-PVD and HVOF for post compacting by hot isostatic pressing, *Powder Metall.*, 2015, vol. 58, pp. 259–264.
17. Aydinöz, M.E., Brenne, F., Schaper, M., Schaak, C., Tillmann, W., Nellesen, J., and Niendorf, T., On the microstructural and mechanical properties of post-treated additively manufactured Inconel 718 superalloy under quasi-static and cyclic loading, *Mater. Sci. Eng. A*, 2016, vol. 669, pp. 246–258.
18. Bambach, M., Sizova, I., Silze, F., and Schnick, M., Hot workability and microstructure evolution of the nickel-based superalloy Inconel 718 produced by laser metal deposition, *J. Alloys Compd.*, 2018, vol. 740, pp. 278–287.
19. Lukina E.A., Bazaleeva K.O., Petrushin N.V., Zai'tcev D.V. Study of formation regularities of the grain structure of the Ni–Al–W–Co–Nb–Cr–Ti–Mo alloy system synthesized by the SLS method depending on parameters of the laser beam, heat treatment, and HIP, in: *Materialy Mezhdunarodnoi nauchno-tekhnicheskoi konferentsii "Beam Technologies and Laser Application"* (Proc. Inter. Sci. and Tech. Conf. "Beam Technologies and Laser Application"), St. Petersburg: St. Petersburg Polytekh. Univ., 2016, pp. 307–315.
20. Bazaleeva, K.O., TCvetkova, E.V., and Balakirev, E.V., Processes of recrystallization of the austenitic alloy fabricated by selective laser melting, *Vestn. MGTU im. N.E. Baumana. Ser. Mashinostr.*, 2016, vol. 111, no. 5, pp. 117–127.
21. Bazaleeva, K.O., Tsvetkova, E.V., Smurov, I.Yu., Yadroitcev, I.A., Bazaleev, E.V., and Kostyuk, Yu.G., Cellular structure in austenitic alloys fabricated by selective laser melting, *Perspekt. Mater.*, 2014, no. 3, pp. 55–62.

Translated by N. Korovin